

## Differential absorption measurements of carbon dioxide using a temperature tunable distributed feedback diode laser

Kevin S. Repasky<sup>a)</sup> and Seth Humphries

*Electrical and Computer Engineering Department, Cobleigh Hall Room 610, Montana State University, Bozeman, Montana 59717*

John L. Carlsten

*Physics Department, EPS Room 264, Montana State University, Bozeman, Montana 59717*

(Received 1 August 2006; accepted 30 September 2006; published online 14 November 2006)

The design and performance of an absorption measurement instrument for monitoring carbon dioxide are presented. The instrument is based on a temperature tunable distributed feedback diode laser capable of tuning between 2.001 and 2.005  $\mu\text{m}$ . Within this wavelength range are 12 absorption lines for carbon dioxide and 9 absorption lines for water vapor. Initial measurements of laser transmission as a function of carbon dioxide concentration are made using a 2 m long absorption cell. The measured values compare well with the expected values using the known line strength of the carbon dioxide absorption feature. Carbon dioxide measurements over a 77.5 m path length made outside the laboratory show the potential for carbon dioxide concentration monitoring. © 2006 American Institute of Physics. [DOI: 10.1063/1.2370746]

### I. INTRODUCTION

The atmospheric concentration of carbon dioxide has grown at a rate of 1.0% per year between 1990 and 1995 and 1.4% per year between 1995 and 2001.<sup>1,2</sup> In 2005, atmospheric concentrations of carbon dioxide increased by 2.6 ppm yielding an average atmospheric concentration of carbon dioxide of 381 ppm.<sup>3</sup> The increasing levels of atmospheric carbon dioxide are partly due to its release through the burning fossil fuels such as coal, oil, and natural gas and through changing land use involving deforestation.<sup>1,4</sup> The increasing level of atmospheric carbon dioxide concentration has potential impacts on Earth's climate.<sup>4</sup> In order to mitigate the effects of climate change due to increasing concentrations of carbon dioxide, emission of carbon dioxide must be reduced. The atmospheric carbon dioxide concentration can be stabilized at 450 ppm by the year 2100 if the total global emissions are reduced by 55%–90%.<sup>5</sup>

Several options for reducing the emission of carbon dioxide are currently being pursued including improved energy efficiency, switching to less carbon-intensive fossil fuels, increased use of alternative energy sources including solar and wind, carbon dioxide sequestration enhancement due to natural biological sinks, and carbon capture and storage.<sup>1</sup> Carbon capture and storage reduces carbon dioxide emission to the atmosphere by first capturing the carbon dioxide generated by the burning of fossil fuels. The captured carbon dioxide is then stored in a geologic site such as a depleted oil well or underground coal seam. Thus the geologic sequestration of the captured carbon dioxide effectively removes atmospheric releases.

Currently, three industrial scale carbon capture and storage projects are operating. The Sleipner Saline Aquifer Stor-

age Project removes  $1 \times 10^6$  tons of carbon dioxide and stores it in a deep subsea brine-filled sandstone formation.<sup>1,6</sup> The Salah Gas Project began in 2004 and is currently storing  $1 \times 10^6$  tons of carbon dioxide in a depleted gas field.<sup>1,7</sup> A third project located in Saskatchewan, Canada is using carbon dioxide captured by the Dakota Gasification Plant located in North Dakota for both enhanced oil recovery and carbon dioxide storage in the Weyburn oil field.<sup>1,8–10</sup> Several smaller pilot projects for carbon dioxide storage are also under investigation.

An important issue to ensure the successful storage of carbon dioxide in geologic sequestration sites is the ability to monitor these sites for leakage.<sup>1,11</sup> The three main causes of leakage include leaking injection wells, improperly sealed abandoned wells, and geologic faults and fractures. Initial studies of geologic storage sites indicate that for carbon storage to be effective, seepage rates must be less than 0.1%–0.01% per year.<sup>1</sup>

Several technologies have been proposed for monitoring carbon storage sites including eddy-covariance,<sup>12–14</sup> flux chambers,<sup>15</sup> and optical methods.<sup>16–19</sup> The optical methods use the fact that carbon dioxide absorbs light at specific wavelengths and the amount of absorbed light can be used to determine the concentration of carbon dioxide. Carbon dioxide has a strong set of absorption lines near 2  $\mu\text{m}$  that affects the amount of transmitted light.<sup>20</sup> The amount of light absorbed by the carbon dioxide can be used to determine the concentration of the carbon dioxide in the local atmosphere to monitor for leakage. In this article, a tunable laser based instrument is described that is capable of tuning over 12 carbon dioxide absorption lines. Molecular concentrations can be ascertained by measuring the amount of absorption and relating this through the line strength of the absorption feature to the concentration of carbon dioxide molecules.

This article is organized as follows. In Sec. II, a relation-

<sup>a)</sup>Electronic mail: repasky@ece.montana.edu

ship between the transmission and atmospheric molecular concentration is developed. The differential absorption instrument for measuring atmospheric concentration of carbon dioxide based on transmission measurements is described in Sec. III. Experimental measurements of carbon dioxide concentrations are described in Sec. IV. Finally, some brief concluding remarks are presented in Sec. V.

## II. RELATING ABSORPTION TO MOLECULAR CONCENTRATION

The amount of light transmitted through a path length  $L$  can be found from the relationship

$$T = \frac{I}{I_0} = e^{-\alpha L}, \quad (1)$$

where  $T$  is the transmission,  $I$  is the optical intensity after the path length  $L$ ,  $I_0$  is the intensity at the beginning of the path, and  $\alpha$  is the absorption per unity length. The optical depth  $\alpha L$  can be written in terms of the molecular line intensity  $S$  and normalized line shape  $g(\nu - \nu_0)$  as<sup>20</sup>

$$\alpha L = Sg(\nu - \nu_0)NP_aL, \quad (2)$$

where  $NP_a$  is the number density of the molecules of interest with  $P_a$  the partial pressure of the molecules of interest. The factor  $N$  scales with temperature and can be written as<sup>20</sup>

$$N = N_L \frac{296}{T_a}, \quad (3)$$

where  $N_L = 2.479 \times 10^{19}$  molecules/cm<sup>3</sup> atm is Loschmidt's number and  $T_a$  is the temperature in Kelvin. The total number density of molecules can be written as  $N_{\text{total}} = N_L P_T$ , where  $P_T$  is the total pressure, while the number density of the molecules of interest can be written as  $N = N_L P_a$ . Thus the concentration of molecules of interest can be written as  $C = N/N_{\text{total}} = P_a/P_T$ . Using this result and Eqs. (1)–(3), an expression for the concentration of the molecules of interest can be written as

$$C = \frac{P_a}{P_T} = \frac{-\ln(T)}{Sg(\nu - \nu_0)N_L(296/T_a)P_T L}. \quad (4)$$

The values for the line intensity and normalized line shape are listed in the HITRAN database for many molecules of interest.<sup>20</sup> A listing of the molecules, wavelengths, line intensities, and normalized line shapes is given in Table I for the wavelength range of 2.001–2.005  $\mu\text{m}$ .

A plot of the transmission as a function of path length for the carbon dioxide absorption line at the wavelengths of 2.001 10, 2.004 02, and 2.004 96  $\mu\text{m}$  is shown in Fig. 1. For this calculation, a total pressure of 1 atm, a temperature of 296 K, and a concentration of 381 ppm were assumed. Using the values given in Table I, values for the absorption per unit length of  $\alpha = 8.89 \times 10^{-4}$ ,  $1.36 \times 10^{-3}$ , and  $1.99 \times 10^{-5}$  m<sup>-1</sup> were calculated for the absorption features at 2.001 10, 2.004 02, and 2.004 96  $\mu\text{m}$ , respectively.

A plot of the transmission as a function of carbon dioxide concentration is shown in Fig. 2 for the absorption feature at 2.004 02  $\mu\text{m}$  for 100, 200, and 500 m path lengths. For this calculation, a total pressure of 1 atm and a temperature of 296 K were assumed. With an initial atmospheric

TABLE I. Absorption features of carbon dioxide and water vapor in the 2.001–2.005  $\mu\text{m}$  spectral region.

Molecule	Wavelength ( $\mu\text{m}$ )	Line intensity ( $10^{-21}$ cm/molecule)	Normalized line shape (cm)
CO <sub>2</sub>	2.001 10	0.811 20	1.1600
H <sub>2</sub> O	2.001 22	0.001 37	1.0916
H <sub>2</sub> O	2.001 28	0.000 66	4.5473
H <sub>2</sub> O	2.001 33	0.000 20	4.6810
CO <sub>2</sub>	2.001 56	0.931 60	1.1516
CO <sub>2</sub>	2.002 03	1.048 00	1.1401
H <sub>2</sub> O	2.002 30	0.009 76	0.8972
CO <sub>2</sub>	2.002 51	1.153 00	1.1304
H <sub>2</sub> O	2.002 83	0.044 90	1.0596
CO <sub>2</sub>	2.003 00	1.241 00	1.1161
H <sub>2</sub> O	2.003 47	0.000 71	1.2960
CO <sub>2</sub>	2.003 50	1.302 00	1.1022
CO <sub>2</sub>	2.004 02	1.332 00	1.0842
CO <sub>2</sub>	2.004 49	0.016 18	1.1754
H <sub>2</sub> O	2.004 49	0.019 09	1.3792
H <sub>2</sub> O	2.004 53	0.006 08	1.4135
H <sub>2</sub> O	2.004 54	0.023 19	0.9622
CO <sub>2</sub>	2.004 54	0.014 63	0.1772
CO <sub>2</sub>	2.004 55	1.322 00	1.0653
CO <sub>2</sub>	2.004 94	0.019 69	1.1703
CO <sub>2</sub>	2.004 96	0.017 96	1.1720

concentration of carbon dioxide of 381 ppm, a 1% decrease in transmission will result when the carbon dioxide concentration changes to 391 ppm (398 ppm, 399 ppm) for the 500 m (200 m, 100 m) path length. This indicated that a measurable change in transmission of 1% will result in an instrument sensitivity of 11 ppm (17 ppm, 18 ppm).

## III. DIFFERENTIAL ABSORPTION INSTRUMENT FOR CARBON DIOXIDE MONITORING

A schematic of the differential absorption instrument used for carbon dioxide monitoring is shown in Fig. 3. A distributed feedback (DFB) diode laser is used as the source

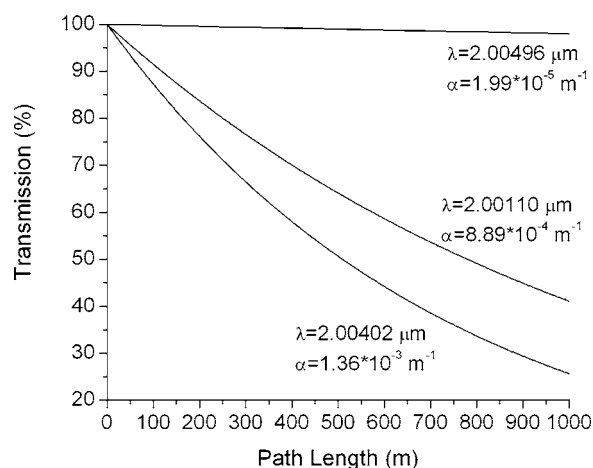


FIG. 1. Predicted transmission as a function of path length for three different absorption lines associated with carbon dioxide. The absorption lines were selected for this plot to demonstrate the variation of line strength as a function of wavelength. The carbon dioxide concentration was assumed to be 381 ppm for this plot.

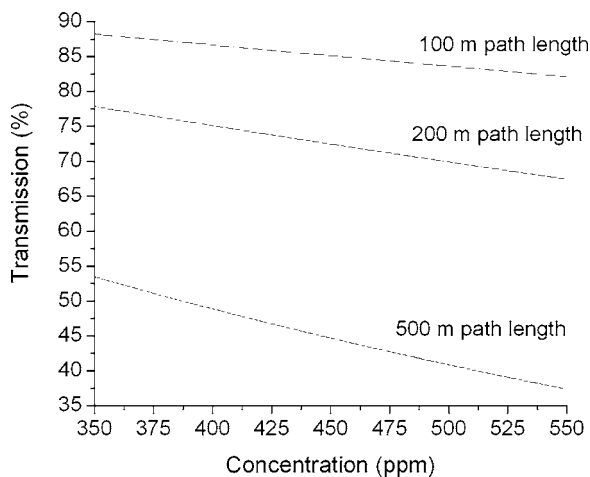


FIG. 2. Predicted transmission as a function of carbon dioxide concentration for various path lengths for one absorption feature.

for this instrument.<sup>21</sup> The laser has a nominal wavelength of  $2.003 \mu\text{m}$  and can be tuned via temperature. The DFB laser is packaged in a sealed TO 8 can with an integrated Peltier cooler for temperature control and thermistor for temperature monitoring. Current is supplied to the diode laser with a commercial current driver while the temperature of the diode is monitored and controlled also with a commercial temperature controller with general purpose interface bus (GPIB) capabilities. The output of the DFB laser is collimated using an antireflection (AR) coated lens. Next, the beam is incident on a wedged pickoff that reflects 4% of the outgoing light through a focusing lens and onto a reference detector. An extended InGaAs detector with a responsivity cutoff of  $2.2 \mu\text{m}$  is used to monitor the outgoing optical power. The detector, placed in a TO can for protection, has a thermoelectric cooler (TEC) used to stabilize the detector temperature. The TO can window is made of sapphire and has an AR coating for  $2 \mu\text{m}$ . The sapphire window surfaces are wedged at  $4^\circ$  to prevent étalon effects. The light that passes through the wedged pickoff exits the instrument and is incident on a corner cube that can be placed to provide the desired optical

path length. Light reflected from the corner cube is directed back through a focusing lens and is incident on a transmission detector that is identical to the reference detector described above. The voltage signal from both the reference and transmission detectors is monitored using a multichannel voltmeter with GPIB capabilities. Data are collected in the following manner. First, the computer sets the operating temperature of the DFB. Next, the reference and transmission detector voltages are read by the computer. The computer steps the temperature to a new value and the process is repeated. A dwell time between the temperature step and the voltage reading allows the laser operating temperature to stabilize and can be set in the data acquisition program. We have found that a 1 s dwell time is enough to allow the laser temperature and hence the laser wavelength to stabilize for small temperature steps. Large changes in the laser operating temperature require longer dwell times.

The flipper mirror shown in Fig. 3 is used to choose as the output of the instrument either the DFB laser or a HeNe laser. Two apertures (not shown in Fig. 3) are centered on the DFB laser beam with the flipper mirror in the down position. The flipper mirror is then placed in the up position and the path of the HeNe beam is adjusted so that the HeNe beam is also centered on the two apertures. In this way, the HeNe beam and DFB laser beam are spatially overlapped and collinear. When the instrument is taken into the field, initial alignment is completed using the HeNe beam because of the difficulty in monitoring the position of a  $2 \mu\text{m}$  laser beam. The flipper mirror is then put in the down position so that the output of the instrument is now the  $2 \mu\text{m}$  beam from the DFB laser. Fine adjustments are made to first maximize the power on the reference detector and then maximize the power on the transmission detector. At this point, absorption measurements can now be made.

#### IV. EXPERIMENTAL MEASUREMENTS

The first issue that needs to be addressed with the differential absorption measurements using the DFB laser is to determine the wavelength tuning characteristics of the DFB laser. The relative tuning rate as a function of temperature was determined using a glass window as an étalon. The glass window has a thickness of 0.953 cm and an index of refraction of 1.53, corresponding to a free spectral range of 10.3 GHz. A plot of the transmission through the optical étalon as a function of temperature is shown in Fig. 4. The laser is tuned through one free spectral range of 10.3 GHz when the detector voltage goes through one period. A tuning rate of 18.9 GHz/C is thus measured for the DFB laser.

The differential absorption instrument was next scanned over several absorption lines of both carbon dioxide and water vapor and the results are shown in Fig. 5. A path length of 77.5 m was used for this measurement. The dashed line represents the normalized transmission determined by dividing the voltage reading from the transmission detector by the voltage reading of the reference detector. The solid line represents the theoretical prediction for the transmission as a function of wavelength using the HITRAN database.<sup>20</sup> The absolute wavelength of the measured transmission was deter-

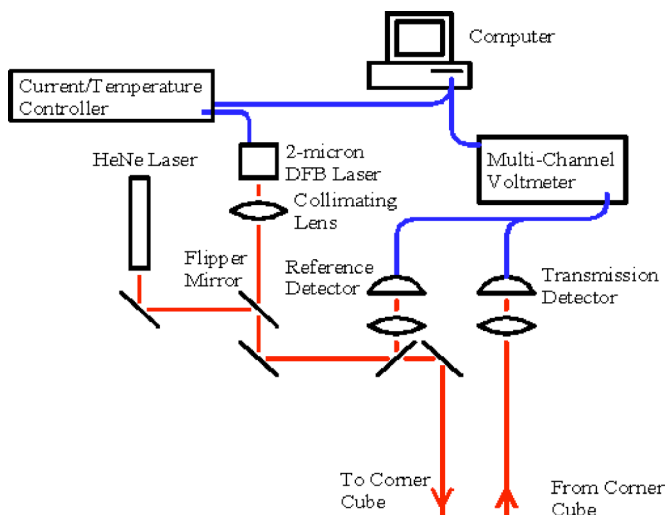


FIG. 3. (Color online) Schematic of the differential absorption instrument used for measurements of atmospheric concentrations of carbon dioxide.

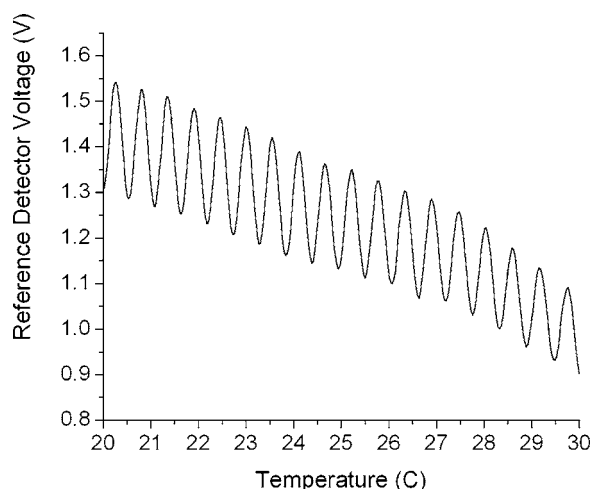


FIG. 4. Optical power as a function of the operating temperature of the DFB laser after an étalon with a free spectral range (one period) of 10.3 GHz. From this figure, a relative tuning rate of 18.9 GHz/C is measured for the DFB laser.

mined by matching the frequency spacing of the measured absorption features using the measured tuning rate of the DFB with the known frequency spacing of the absorption features using the HITRAN database. Good agreement is seen between the measured and predicted transmission spectra.

The ability to predict molecular concentrations of carbon dioxide was next studied using a 2 m long pressure cell. The experimental setup is shown schematically in Fig. 6. The output from the differential absorption instrument is directed through a 2 m long pressure cell. The transmission detector was removed from the instrument and placed directly behind the pressure cell, providing a path length of 2 m.

Data are taken in the following manner. First, the pressure cell is evacuated using a roughing pump. Next, a small amount of carbon dioxide is allowed to enter the chamber and a pressure reading is taken using a pressure sensor (Mensor Series 6100). Nitrogen was next introduced into the pres-

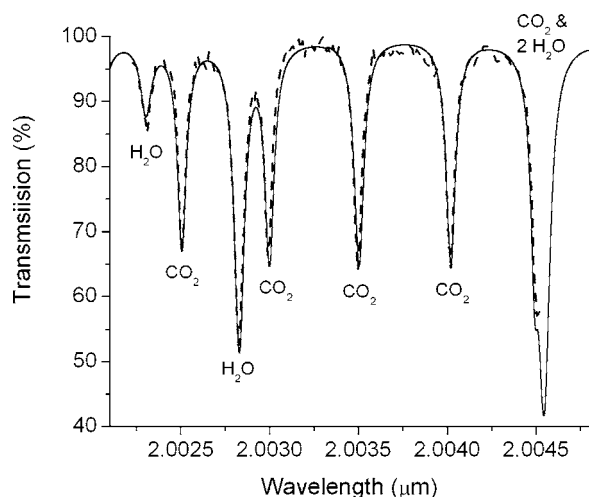


FIG. 5. Transmission as a function of wavelength for an open-air path length of 77.5 m. The dashed line represents the measured transmission spectrum using the differential absorption instrument while the solid line indicates the predicted transmission spectrum using the HITRAN database.

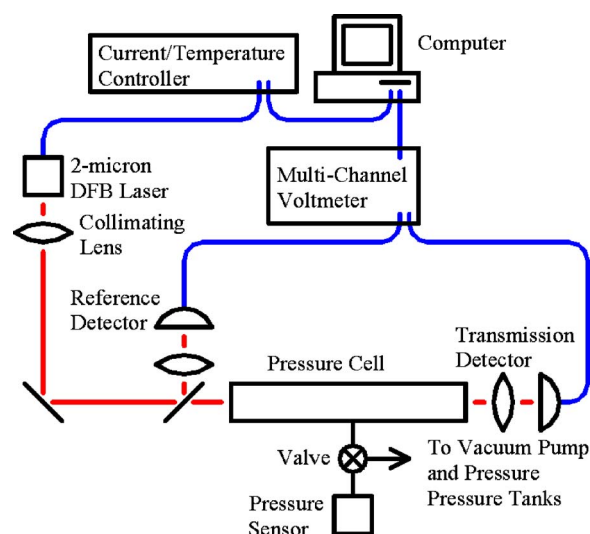


FIG. 6. (Color online) Schematic of the experimental calibration setup used for measuring transmission as a function of carbon dioxide concentration.

sure cell so that the total pressure within the cell was approximately 1 atm and a second pressure reading was taken. The concentration within the cell of carbon dioxide can be calculated by taking the ratio of these two pressures. The laser was next scanned across an absorption feature and the transmission through the cell was measured as a function of wavelength. This process was repeated using several different carbon dioxide concentrations. A plot of the transmission as a function of carbon dioxide concentration for a 2 m path length is shown in Fig. 7. The solid line indicated the expected results while the solid circles represent the measured values using the technique described above. The error bars associated with the measured values are attributed to the accuracy of the pressure sensor. Good agreement with the predicted and measured results are seen in Fig. 7, indicating carbon dioxide concentrations can be accurately measured using this differential absorption instrument.

## V. DISCUSSION

The design and performance of a differential absorption instrument for monitoring atmospheric concentrations of car-

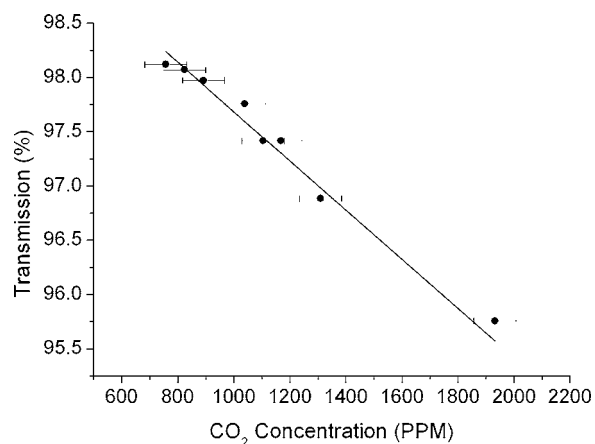


FIG. 7. Transmission as a function of carbon dioxide concentration. The solid line represents the predicted values while the solid circles represent the measured values. The error bars indicate the accuracy of the pressure sensor used to measure carbon dioxide concentrations.

bon dioxide were presented. This instrument is based on a temperature tunable DFB laser with a center wavelength of 2.003  $\mu\text{m}$  and a measured tuning rate of 18.9 GHz/C. The DFB laser is capable of tuning from 2.001 to 2.005  $\mu\text{m}$ . This spectral region has several carbon dioxide and water vapor absorption lines of varying strength that allow the user to choose an absorption line so that varying path lengths can be monitored effectively. The pressure cell measurements indicate that differences in transmission of 1% can be measured with this instrument, indicating that for a 500 m (200 m, 100 m) path length for the carbon dioxide absorption line at 2.004 02  $\mu\text{m}$ , the instrument can measure carbon dioxide concentration changes of 2.9% (4.5%, 4.7%). Temperature effects on the transmission can be determined by scanning across more than one carbon dioxide absorption line and can thus have a minimal effect on the atmospheric carbon dioxide concentration measurements. The instrument described in this article has the potential for providing an optical detection scheme for monitoring the integrity of carbon diode storage sites, thus providing a needed piece of technology for successful carbon sequestration.

## ACKNOWLEDGMENTS

This work was kindly support by the Department of Energy under Award No. DE-FC26-04NT42262. However, any opinions, findings, conclusions, or recommendations expressed herein are those of the author(s) and do not necessarily reflect the views of DOE.

<sup>1</sup>*Intergovernmental Panel on Climate Change Special Report on Carbon Dioxide Capture and Storage*, edited by B. Metz, O. Davidson, H. de

Coninck, M. Loos, and L. Meyer (Cambridge University Press, Cambridge, UK, 2005).

<sup>2</sup>K. Masarie and P. P. Tans, *J. Geophys. Res.* **100**, 1593 (1995).

<sup>3</sup>P. P. Tans, National Oceanic and Atmospheric Administration, 2006 <http://www.cmdl.noaa.gov/ccgg/trends/>.

<sup>4</sup>*Climate Change 2001. Synthesis Report. A Contribution of Working Groups I, II, and III to the Third Assessment Report of the Intergovernmental Panel on Climate Change*, edited by R. T. Watson (Cambridge University Press, Cambridge, UK, 2001).

<sup>5</sup>*Climate Change 2001—Mitigation. The Third Assessment Report of the Intergovernmental Panel on Climate Change*, edited by B. Metz, O. Davidson, R. Swart, and J. Pan (Cambridge University Press, Cambridge, UK, 2001).

<sup>6</sup>R. Korbol and A. Kaddour, *Energy Convers. Manage.* **36**, 509 (1995).

<sup>7</sup>This project is described at [www.bp.com](http://www.bp.com)

<sup>8</sup>S. Whittaker, *Can. Soc. Petrol. Geol. Reservoir* **31**, 9 (2004).

<sup>9</sup>S. G. Whittaker, K. Kreis, T. L. Davis, Z. Hajnal, T. Heck, L. Penner, H. Qing, and B. Rostron, Proceedings of the Diamond Jubilee Convention of the Canadian Society of Petroleum Geologists, 2002 (unpublished).

<sup>10</sup>D. Mingzhe, L. Zhaowen, L. Shuliang, and S. Huang, *Energy Convers. Manage.* **47**, 1372 (2006).

<sup>11</sup>S. M. Benson, E. Gasperikova, and G. M. Hoversten, Proceedings of the seventh International Conference on Greenhouse Gas Control Technologies (GHGT-7), 2005 (unpublished), pp. 1259–1266.

<sup>12</sup>K. J. Davis, P. S. Bakwin, C. Yi, B. W. Berger, C. Zhaos, R. M. Teclaw, and J. G. Isebrands, *Global Change Biol.* **9**, 1278 (2003).

<sup>13</sup>D. D. Baldocchi, *Global Change Biol.* **9**, 479 (2003).

<sup>14</sup>D. P. Billesbach, M. L. Fischer, M. S. Torn, and J. A. Berry, *J. Atmos. Ocean. Technol.* **21**, 639 (2004).

<sup>15</sup>N. T. Edwards and J. S. Riggs, *Soil Sci. Soc. Am. J.* **67**, 1266 (2003).

<sup>16</sup>T. J. Griffis, J. M. Baker, S. D. Sargent, B. D. Tanner, and J. Zhang, *Ag. Forrest Meteorol.* **124**, 15 (2004).

<sup>17</sup>Y. Yoshii, H. Kuze, and N. Takeuchi, *Appl. Opt.* **42**, 4362 (2003).

<sup>18</sup>P. Powers, T. J. Kulp, and R. Kennedy, *Appl. Opt.* **39**, 1440 (2000).

<sup>19</sup>G. J. Koch *et al.*, *Appl. Opt.* **43**, 5092 (2004).

<sup>20</sup>L. S. Rothman *et al.*, *J. Quant. Spectrosc. Radiat. Transf.* **82**, 5 (2003).

<sup>21</sup>The 2  $\mu\text{m}$  DFB laser was purchased through Nanoplus ([www.nano-plus.com](http://www.nano-plus.com)).